Analyzing Simulated Very High Energy Gamma-ray data from Dark Matter Annihilation
REU Program at Columbia University - Nevis Labs

Alex Sidler[1]

[1]Grinnell College

August 5, 2024

Nevis Laboratories
Columbia University

INTERNAL DOCUMENT
NOT FOR DISTRIBUTION

Abstract

Over the summer, I studied very high energy gamma-ray detection and analysis using the Cherenkov Telescope Array Observatory's (*CTAO*'s) second science data challenge. I learned about cosmic rays, cosmic accelerators, and the processes that create gamma rays including synchrotron radiation and inverse-Compton scattering. I studied how gamma rays interact with the atmosphere and, through Bremsstrahlung, create air showers of charged particles. By moving faster than light in the medium, these charged particles create Cherenkov radiation that IACTs can then detect. These tools to observe gamma rays can be used to detect dark matter indirectly. In some models, weakly interacting charged particles (WIMPs) are compelling candidates for dark matter (DM) where gamma rays may be produced as a result of DM annihilation. The dark matter emits gamma rays either promptly, as a direct product of the dark matter annihilation, or secondarily, as emissions from standard model particles produced by dark matter annihilation. For this reason, it is important that we build more sensitive detectors like the *CTAO*. While the *CTAO* is still under construction, we can pave the way for the data analysis pipeline now using the simulated science data challenge data. My project consists of analyzing three dark matter sources: the dwarf spheroidal galaxies Willman-1 and Sagittarius-2, and a galactic dark matter subhalo. We establish an analysis pipeline using the well-studied active galactic nucleus source Markarian-421 as a verification source. We start with background estimation, using both ring and reflected regions techniques to model the background. Then, we approximate flux spectra and significance maps using a combination of forward-folding and backward-folding methods. We compare our resulting flux spectrum with *VERITAS* and *Fermi-LAT* data. Finally, we go through the same analysis pipeline for the three dark matter sources. We find no evidence of gamma-ray emissions from Sagittarius-2 or the dark matter subhalo. However, we do find a 5.4σ significance gamma-ray detection from Willman-1. On further analysis, the significance distribution for the Willman-1 source shows that the analysis was likely marred by error, so further debugging and differing analytical approaches will be required to verify the Willman-1 results.

Contents

1 Introduction & Background **2**

1.1 Very High Energy Gamma Ray Detection 2

1.2 CTAO and the Second Science Data Challenge 3

1.3 Dark Matter 4

2 Analytical Methods **6**

2.1 Gammapy and SDC data 6

2.2 Instrument Response Functions 6

2.3 Background Estimation 7

2.4 Modeling, Fitting, and Estimators 8

3 Results **9**

3.1 Markarian-421 9

3.2 Sagittarius 2 11

3.3 Dark Matter Subhalo 11

3.4 Willman-1 12

4 Summary and Conclusions **14**

5 Acknowledgements **15**

1 Introduction & Background

1.1 Very High Energy Gamma Ray Detection

One of the oldest unsolved mysteries in astrophysics is the origin of the highest energy cosmic rays in the universe. Cosmic rays are charged particles that come from space and interact with the earth's atmosphere. As shown in Fig. 1, Cosmic rays can have a wide range of energies, from < 1GeV to $> 10^9$GeV [20]. In 1991, the highest energy cosmic ray ever detected was measured to be traveling at a speed 0.9999999999999999999999951 times the speed of light and have an energy of 10^{20}eV. High-energy cosmic rays come from astrophysical power sources that accelerate

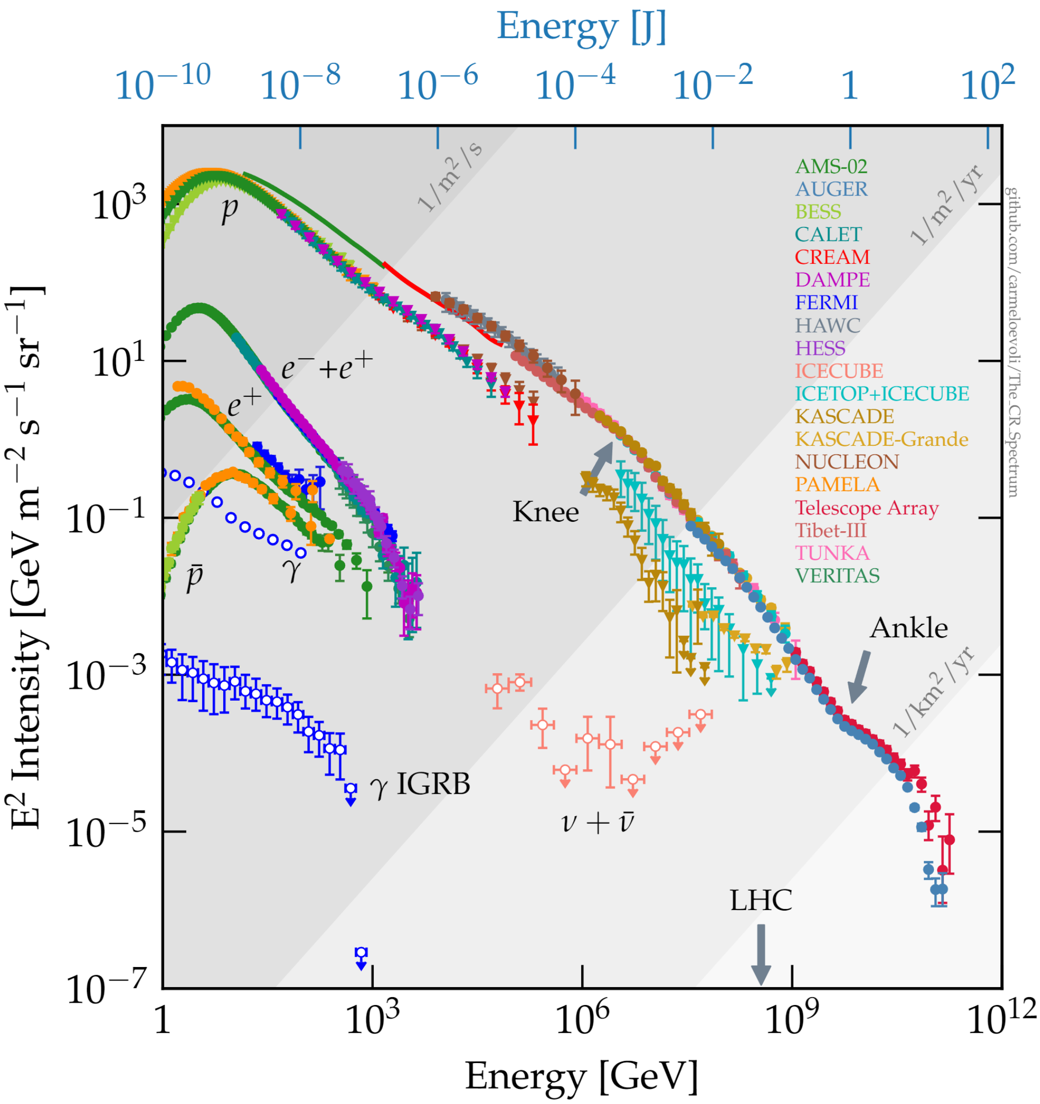

Figure 1: *The cosmic ray energy intensity spectrum [20].*

charged particles through electromagnetic or gravitational processes. These accelerators consist of rotating, highly magnetized objects like pulsars, as well as gravitationally powered objects like supernovae remnants, black holes, and neutron stars. However, the processes that create these ultra high energy (UHE) cosmic rays are still being understood. Unfortunately, UHE cosmic rays are difficult to study because we cannot effectively trace UHE cosmic rays back to their source accelerators. This is because cosmic rays are significantly deflected by interstellar and intergalactic magnetic fields. By the time they reach Earth, they will have been greatly and unpredictably deflected from their initial trajectory. However, through processes like synchrotron radiation and inverse-compton scattering, the same accelerators that emit cosmic rays also emit X-rays and gamma rays. Unlike cosmic rays, we can trace these very high energy (VHE) gamma rays back to their source astrophysical accelerators. This allows us to indirectly detect and study high-energy cosmic particle accelerators, locations where cosmic particle densities are high, and places where relic particles collect. Therefore, VHE gamma rays are the key to detecting and analyzing the astrophysical accelerators that give cosmic rays such high energies.

We can observe VHE gamma rays through ground-level observatories by the Cherenkov radiation they produce in the atmosphere. When VHE gamma rays interact with the atmosphere, they produce extensive electromagnetic cascades called "air showers" through pair-production and Bremsstrahlung. These air showers generate short-lived but intense flashes of Cherenkov radiation that we can detect using imaging atmospheric Cherenkov telescopes (IACTs) [32]. Because of this, we can observe very high energy gamma rays using ground-based IACTs such as those being used in the Very Energetic Radiation Imaging Telescope Array System (*VERITAS*) and the Cherenkov Telescope Array Observatory (*CTAO*) [32] [23].

1.2 CTAO and the Second Science Data Challenge

My research focuses on the *CTAO* and its future utility as a cutting-edge instrument for imaging air showers. The *CTAO* is a project that aims to implement next-generation ground-based IACTs in two new facilities in the northern and southern hemispheres [23]. Capable of full-sky coverage, unparalleled sensitivity, and, as shown in Fig. 2, a wide gamma-ray energy coverage from 20 GeV to 300 TeV, the *CTAO* will be ground-breaking for the field of gamma-ray astronomy and astrophysics [23]. Furthermore, the *CTAO* will be a great candidate for observing

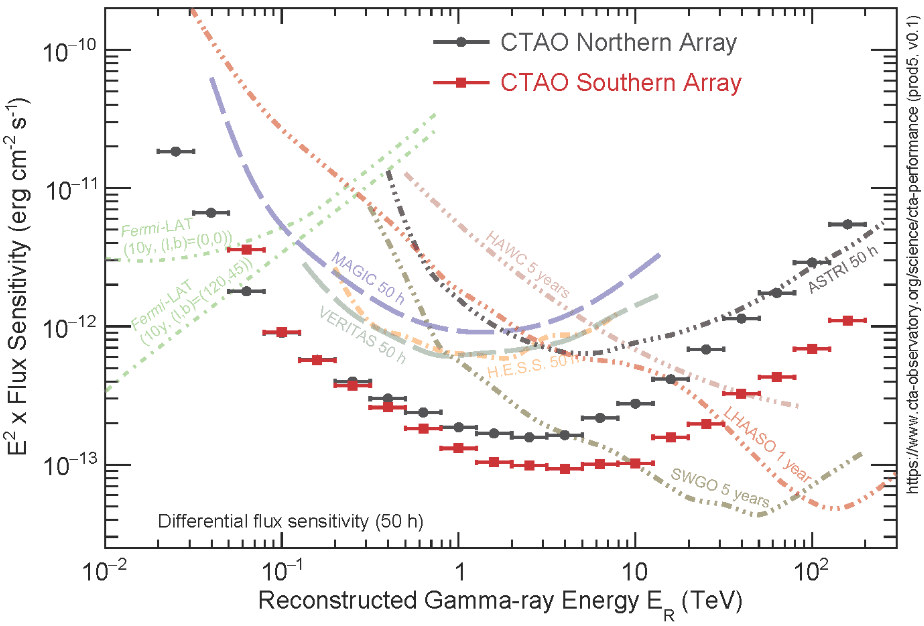

Figure 2: *The CTAO's expected differential sensitivity, defined as the minimum flux needed by CTAO to obtain a 5-standard-deviation detection of a point-like source [23]. The CTAO's performance is compared with other high-energy and very-high-energy gamma-ray instruments [28] [8] [5] [1] [24] [14] [6] [32].*

multi-messenger astronomical events. As the most sensitive VHE gamma-ray detector, the *CTAO* will be able to follow up on time-sensitive event detection with a unique astrophysical perspective [23]. Because of this, it is integral that we develop a sound and robust channel for data flow and data analysis to make full use of the *CTAO*'s capabilities. This is the goal of the second Science Data Challenge (SDC) and my project over the course of the summer. I aim to test Gammapy, an open-source data analysis tool [19] [2], and to develop a data-analysis workflow using the SDC's simulated datasets.

Gammapy is a science analysis package for Python that was developed as a tool to analyze output *CTAO* data [23]. Gammapy is open-source and will be used by the greater community as a data analysis tool. However, Gammapy is still a relatively new package and we must learn how to effectively use it. This is the general aim of the SDC. The SDC is a series of simulated *CTAO* output datasets designed to be used with Gammapy. My project for the summer of 2024 consists of using gammapy to analyze galactic and extragalactic dark-matter-heavy gamma-ray sources given in the SDC. I will document my results and my experience with gammapy along the way with the aim of providing feedback and developing a robust data-analysis workflow that will assist others in their use of Gammapy.

1.3 Dark Matter

Furthermore, this project will allow me to gain a greater understanding of indirect dark matter (DM) searches. The identity and nature of dark matter is still unknown, but there is much observational evidence to support its existence. For example, the rotation curves of galaxies disagree with what we expect from Newtonian gravity [21]. As illustrated in Fig. 3, the observed velocities are constant out to large radii instead of decreasing with distance from the galactic center. Our standard understanding of gravity says that, at such velocities, the outer mass of the galaxy should escape the galaxy's gravitational pull. Because of this, we infer that there is some invisible "dark" mass binding the galaxy together.

Analyzing gamma-ray emissions from DM sources is important because we can indirectly detect DM self-annihilation or decay [15]. By assuming dark matter in the form of weakly interacting massive particles (WIMPs), we can attempt to detect the gamma-ray emissions of some self-annihilation or decay channels. While not the only possible model for dark matter, a several-GeV-to-few-TeV scale WIMP is convincing and is often considered the most likely dark matter candidate [15]. This is due to the predicted weakly-interacting relic abundance being equal to the observed DM abundance [15] [31]. WIMP annihilation or decay into standard matter (SM) through a few primary channels would produce energies on a similar scale to VHE gamma-rays or charged particles. Thus, dark matter annihilation or decay (DMAD) will emit high-energy and VHE gamma rays, through prompt emission directly from DMAD or by standard inverse-comption and hadronic processes from resulting energetic charged particles.

The sources I examined for this analysis include the dwarf spheroidal galaxies Willman-1 and Sagittarius-2 3.4 3.2, the high-synchrotron peaked blazar (HBL) Markarian-421 3.1, and a galactic dark-matter subhalo 3.3. Markarian-421 is one of the brightest and most studied extragalactic sources of TeV gamma rays [17]. It has a redshift of $z = 0.031$ and was first observed by the Whipple observatory in 1992 [34]. Because the source is well-studied, and of its known redshift, spectrum, and model [17], I can analyze Markarian-421 data as a verification source for the data analysis pipeline and compare my spectrum with known values. Dwarf spheroidal galaxies are good source candidates for dark matter due to their high mass-to-luminosity ratio [21]. Willman-1 is an ultra-low luminosity dwarf-spheroidal satellite galaxy [36] with a redshift of $z = -0.000043 \pm 3.00e - 6$ [36]. Despite its incredibly low mass of $3.9^{+2.5}_{-1.6} \times 10^5 M_\odot$, its mass-to-light ratio of 770^{+930}_{-440} is very high [36]. This makes Willman-1 an ideal candidate for dark matter detection, as it has a high concentration of dark matter and very few SM sources of luminosity. Sagittarius-2 is a more unknown source. At first, Sagittarius-2 was assumed to be another ultra-low luminosity dwarf spheroidal galaxy [26] [30]. It was believed that Sagittarius-2 is one of the most compact dwarf galaxies in its luminosity range [26] and, like Willman-1, has a very high mass-to-light ratio [26], making it a good candidate for dark matter searches. However, further analyses suggest that Sagittarius-2 may be an extended globular cluster [29]. Furthermore, a reanalysis of the source's makeup suggests that Sagittarius-2 is less DM dependent than we thought [29].

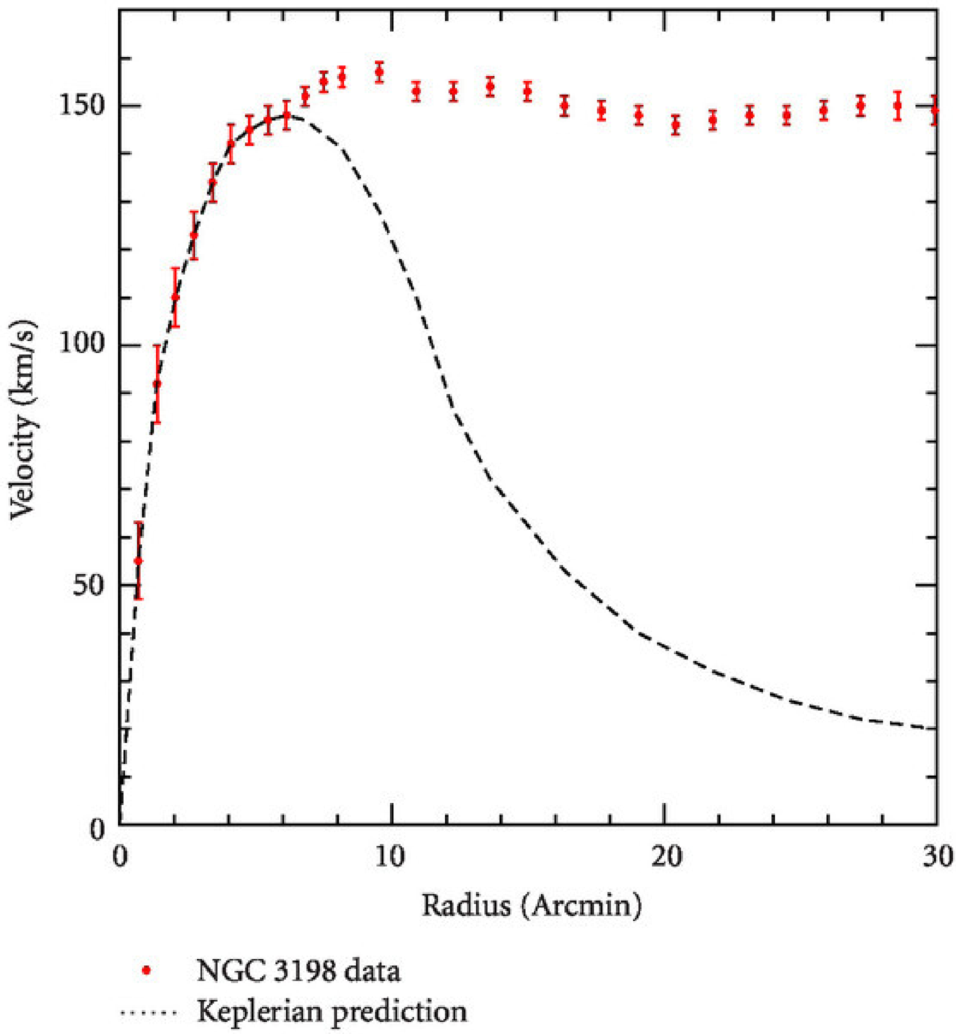

Figure 3: *The measured rotational velocities of NGC 3198 compared to theoretical values [21].*

Gamma-ray analyses from *VERITAS* [9] and *Fermi-LAT* [7] yield no evidence for gamma-ray emission from either Willman-1 or Sagittarius-2. The final source examined is a galactic dark matter subhalo. DM subhalos, as described by [33], are radial substructures of varying DM density within the Milky Way's DM halo [33]. These subhalos would be good candidates for dark matter because of their very high DM to SM mass ratios, meaning that any gamma-ray emissions from the subhalo could only be from DMAD [33].

While *VERITAS* has looked at DM-heavy dwarf spheroidal galaxies [4] and galactic DM subhalos [33] as VHE gamma ray sources in the past, they have found no evidence of indirect DM detection. *VERITAS* was then able to place new limits on the WIMP's annihilation/decay cross section [33]. However, it is possible that, with *CTAO*'s increased sensitivity, future investigations may see observations of VHE gamma-ray emissions from DMAD. At the very least, the *CTAO*'s unparalleled sensitivity will allow us to further constrain the upper limits of the WIMP's cross section.

This outlines my central goal during the summer. I hope to analyze DM-heavy gamma-ray sources using Gammapy. I then create significance maps to confirm gamma ray emissions beyond cosmic ray background, and, if there is a source detection, create 1D flux spectrums of each source. With this, I aim to define a data analysis pipeline for gammapy that will serve as a guide to analyzing dark matter sources in the future.

2 Analytical Methods

2.1 Gammapy and SDC data

Gammapy is an open-source, community-developed Python package designed for use in gamma-ray astronomy [19] [2]. Gammapy is built on other Python packages such as Numpy [22], Scipy [35], and Astropy [12] [10] [11], and is the core library for science data analysis by *CTAO* [23]. Because *CTAO* is being built with the intention of open use by a wide range of scientists, it is important that Gammapy, the data analysis package used by *CTAO*, is well-developed, thoroughly detailed, and effectively documented. Because of this, I developed and tested the Gammapy data analysis pipeline using simulated *CTAO* data through the SDC. While the SDC data will be available to the public in the future, it is important to note that the SDC data is internal and not yet for public release. The SDC data consists of fully calibrated, event-level data in FITS format (data-level 3). These data contain reconstructed gamma-ray directions and energies, instrument response functions for deriving sky maps and gamma-ray spectra, and corresponding indices to maintain a consistent file-system. These data given by the SDC are supposed to simulate the same kind of data users will receive by the *CTAO* [23]. I was provided the SDC data by Dr. Ruo Yu Shang, who himself received the data from Paolo Da Vela and other members of the SDC technical team. Typical data level 3 IACT data are in the form of "observations", which depict particular time frames in which the instrument response is stable [19] [2]. The data I focused on were the active galactic nucleus long-term-monitoring (AGN-LTM) Markarian-421 event data consisting of 118 observations over a livetime of 14 hours, dwarf spheroidal galaxy Willman-1 event data consisting of 181 observations over a livetime of 50 hours, dwarf spheroidal galaxy Sagittarius-2 event data consisting of 125 observations over a livetime of 45 hours, and two galactic dark matter halo sources consisting of 41 and 51 observations, and both with livetime of 50 hours.

2.2 Instrument Response Functions

In high-level gamma-ray data, we assume that the instrument response can be simplified to be the product of three independent functions:

$$R(p, E_{|p_{true}}, E_{true}) = A_{eff}(p_{true}, E_{true}) \times PSF(p_{|p_{true}}, E_{true}) \times E_{disp}(E_{|p_{true}}, E_{true}), \tag{1}$$

where $A_{eff}(p_{true}, E_{true})$ is the effective area function, $A_{eff}(p_{true}, E_{true})$ is the point-spread function, and $E_{disp}(E_{|p_{true}}, E_{true})$ is the energy dispersion function. The instrument response functions (IRFs) given by the SDC consist of simulated effective area data, energy dispersion data, and point spread function data for the instruments. Each of the IRFs are calculated from simulated event reconstruction, for which the true energy E_{true} and position p_{true} of the incident gamma-ray are compared with the reconstructed energy E and position p [19] [2]. The effective area describes the effective collection area of the detector. It is the product of the detector's total collection area, the detection efficiency at a given true energy E_{true}, and the detection efficiency at a given true position p_{true}. The point-spread function is the probability of reconstructing a particular direction p when the true direction is p_{true} and true energy is E_{true} [19] [2]. Similarly, energy dispersion is the probability of reconstructing a particular energy E with a true direction p_{true} and energy E_{true}. The PSF and energy dispersion can be thought of as the spatial and energy resolution of the instrument [19] [2]. Ideally, the PSF and energy dispersion approach unity as p and E approach p_{true} and E_{true}, respectively [19] [2]. The IRFs are used for a variety of techniques during the data analysis process, such as calculating the expected number of events, deriving the background approximation, and estimating flux spectra.

2.3 Background Estimation

To convert from data level 3 to data level 4, we must convert the data to binned, background-reduced datasets. To do this, we start by performing a 5° cut around the source to isolate the observations we will analyze. We then interpolate a logarithmic energy axis from provided energy bounds. Derived from the energy ranges the *CTAO* is capable of taking, we use energy bounds of 0.01 TeV to 300 TeV [23] with 10 bins per decade. This will be the binning of the reconstructed events and the binning of the final maps. We then define the energy axis for the reduced IRF and model binning. This "true energy" axis will have a larger energy range than that of the reconstructed energy axis to avoid background cutoffs [19] [2]. For the true energy axis, we interpolate the same axis as the reconstructed energy axis but extend the energy bounds to be from 0.005 TeV to 600 TeV.

Then, we perform the data reduction process to estimate a background and convert the data to reduced datasets. In gamma-ray analysis, the background comes from deflected VHE cosmic rays. Therefore, to isolate the gamma-ray signals in the data, we need to subtract the cosmic-ray background. During the data reduction process, our goal is to estimate the excess counts from total counts and a modeled background. To estimate background, we examine a patch of empty sky, known as the OFF region. From this OFF region, we extrapolate background counts for the entire observational FoV. We then subtract the estimated background counts from the counts in the integration region, known as the ON region, to determine an excess.

$$N_{excess} = N_{ON} - \alpha N_{OFF} \tag{2}$$

Equation 2 shows the excess counts (N_{excess}) calculation, where N_{ON} are the ON counts, N_{OFF} are the OFF counts, and α is a normalization factor that accounts for differences between the source region and the empty region. Using this excess, we can calculate the significance and flux spectrum of the source.

To estimate background, we use a variety of techniques. The first is during observational data collection. One way to collect ON/OFF data is to spend half the observation time looking at the source while the other half is spent looking at empty space at an equal zenith angle (to maintain consistency). You can then directly subtract the OFF data from the ON data to eliminate background. However, the drawback is that only half the observational time is spent looking directly at the source. One way to avoid this problem is to use the *wobble* technique, pioneered by the HEGRA collaboration [16]. This technique involves keeping the source in the FoV during the entire observational period, but alternating, or 'wobbling', the offset relative to the source's position (typically ± 0.5 deg) [13]. A background estimate can then be made from the empty part of the FoV (the section that does not include the source region or any ON data) [13]. For this analysis, a wobble of ± 0.7 deg in right ascension and declination is used for all sources 3.1 3.4 3.2 except the DM halo source, which does not use a wobble 3.3. Furthermore, we will use multiple background models for different purposes. The two background models we will use are a ring background model and a reflected regions background model, and we will use them for significance maps and flux spectra, respectively. The ring background model involves using a solid ring around the source position as the OFF region [13] [3]. The inner and outer radii of the ring are $r_{inner} = r_{offset} - r_{ON}$ and $r_{outer} = r_{offset} + r_{ON}$, where r_{offset} is the ring's offset radius (often the same as the wobble radius) and r_{ON} is the radius of the ON region [3]. While this technique is applicable to every point in the FoV, an extra acceptance correction function must be used to derive the normalization α for each position on the ring [13]. This is because the ring's segments vary in their offset from the source position [13]. For this analysis, the ring backgrounds we use will have an inner radius of 0.6 deg and a width of 0.2 deg. This corresponds to an ON radius of 0.1 deg. The ring background method is the most robust background estimation method for weak sources detection [13]. Because of this, we use the ring background method for deriving significance maps. An example of a ring background can be seen in Figure 4 (left).

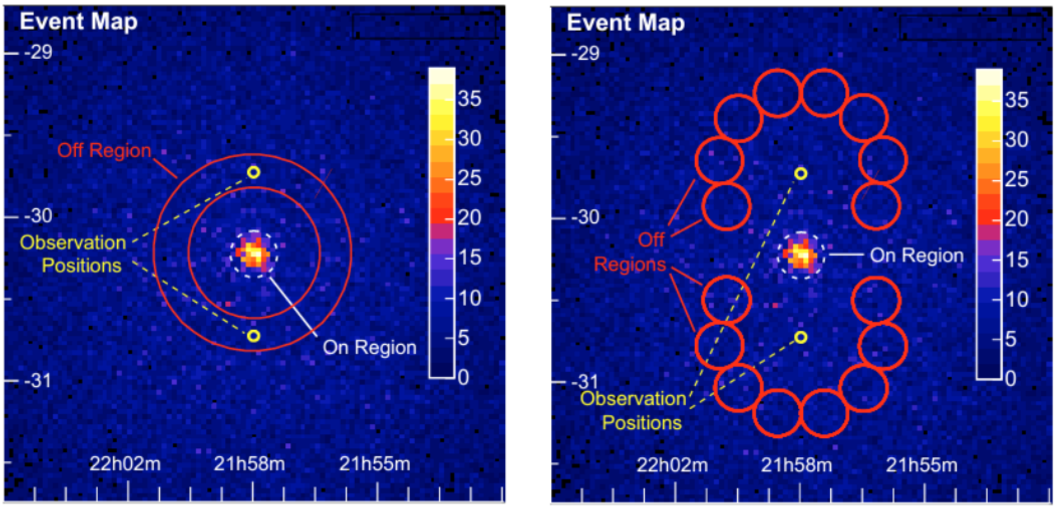

Figure 4: *A visualization of the ring background ON/OFF regions (left) and the reflected region background ON/OFF regions (right). Note that this visualization includes a* $\pm 0.5\,\mathrm{deg}$ *declination wobble. Image courtesy of Berge, Funk, and Hinton [13].*

The reflected regions background can be applied to any point in the FoV besides the observation position [13]. For each observation position, a ring of n_{off} concentric OFF regions are used [13]. These OFF regions are identical in size and shape to the ON region, and are equidistant from the observation position [13]. Any observation positions or OFF regions inside an exclusion region are not used during the analysis [3]. Then, due to the equal offset for each reflected region, no radial acceptance correction is necessary and the normalization α is just $\frac{1}{n_{off}}$. An example of a reflected regions background can be seen in Figure 4 (right).

For this analysis, we use the ring background method for deriving significance maps and we use the reflected regions background method for estimating flux spectra. Furthermore, for the ring background method we use a combination of point-source (integration radius $\approx 0.07\,\mathrm{deg}$) and slightly-extended source (integration radius $\approx 0.10\,\mathrm{deg}$) analysis [3]. For the spectral analysis, we use only the slightly-extended source integration radius of $0.10\,\mathrm{deg}$. Furthermore, we define a safe mask for the background estimation. For the ring estimator, we use a maximum offset of $3.5\,\mathrm{deg}$ and for the reflected regions estimator, we use a maximum effective area of 2% to maximize the spectral band we can estimate over. Furthermore, we use an exclusion mask to remove from the analysis any other known gamma-ray sources within the observational FoV. After the safe mask and exclusion regions are applied, we estimate the background and subtract it from our datasets. This returns reduced datasets with background estimates, α values, and excess counts.

2.4 Modeling, Fitting, and Estimators

After we perform background estimation and subtraction, we fit models and estimators to our reduced datasets to create flux spectra and significance maps. To create significance maps, we convolve the IRFs over a correlation region within the reduced map datasets. For significance analysis, we use backward folding, also known as the Li-Ma formalism and is described in [27]. We use Li and Ma's analytical solution [27] to estimate the significance. In this case, the excess over the null hypothesis determine the "best fit" flux and significance [27]. Once correlated, we can construct significance maps to determine whether or not we detect gamma-rays from the source beyond background. We choose to use backward folding over forward folding because it gives us a (mostly) model-independent significance [27]. However, for the flux spectra we perform forward-folding flux estimation, in which we determine a model, optimize the parameters to fit it to the data, and derive a flux spectra from that fit [19] [2]. For this analysis, we use a combination of standard power law models (PWL) and exponential cutoff power law models (ECPL) to analyze various spectra. These models are shown by Equations 3 and 4, respectively. The optimized parameters and fit statistic (wstat) for each model can be found in 1. The ECPL model for Markarian-421 was taken from [17]. In addition, we multiply the Markarian-421 model with an extragalactic background light (EBL) normalization factor to model EBL spectral absorption. Using the Dominguez EBL model [18], we correct the optimized Markarian-421 model to account for background spectral absorption for a source with a redshift $z = 0.031$. Furthermore, we use the MINUIT [25] backend for model fitting, and we use Gammapy's [19] [2] algorithms to estimate flux points.

$$\phi(E) = \phi_0 \cdot \left(\frac{E}{E_0}^{-\Gamma}\right) \tag{3}$$

$$\phi(E) = \phi_0 \cdot \left(\frac{E}{E_0}^{-\Gamma}\right) \exp(-(\lambda E)^{\alpha}) \tag{4}$$

Source	**Model**	ϕ_0 **(TeVˆ1 sˆ1 cmˆ2)**	Γ	λ (TeV-1)	E_0 **(TeV)**	**wstat**
MRK-421	ECPL	1.0505e-10	1.7854	1.0559	1.0000	3.36
Will-1	ECPL	1.1651e-13	.51718	.48791	1.0000	2.93
Sagi-2	PWL	6.0138e-16	3.8909	N/A	1.0000	3.72
Subhalo	PWL	1.3996e-14	2.8807	N/A	1.0000	3.68

Table 1: *Optimized parameter values and wstat values for power law models fitted to source spectrums.*

After flux estimation, we also calculate flux (TeV cmˆ2 sˆ1) values by hand for multiple flux bins. We do this using the gamma-ray counts (excess counts) estimated by the data reduction process, the effective area for that particular energy as calculated by the IRFs, and the livetimes of the observations. We average the gamma-ray count, effective area values, and livetimes over every observation.

It is important to note that we lack a trial factor estimation or correction, so background significance and upper limits will be somewhat inflated in each graph. Further analysis will be required to show more exact statistical results, but even from these preliminary results we can make some simple conclusions. Furthermore, these results will be useful for comparison with other data analysis pipelines and techniques.

3 Results

3.1 Markarian-421

For Markarian-421, we performed a spectral and significance analysis using the methods described in 2. For Markarian-421, we only perform an analysis using a point-source integration radius and correlation radius. Figures 5a and 5b display the significance plot and related OFF significance distribution, respectively. Plotting the significance distribution outside the source region is important as a check that the background estimation does not contain stray gamma-ray events. This can happen when the ON region(s) are not large enough or when there is a different gamma-ray source in the FoV. Typically, we want the OFF significance distribution to be a standard normal distribution. Markarian-421's OFF distribution is a good example of this. The ON region looks strange because the plot is cut off at 10σ, despite the significance being on the scale of a few hundred, as shown by the significance plot in Figure 5a.

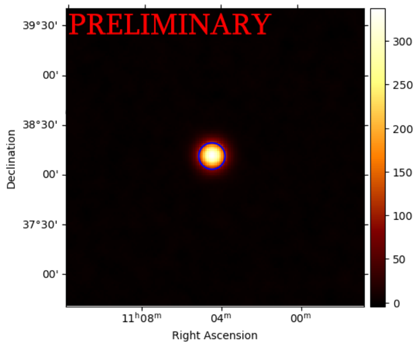

(a) Markarian-421 significance map.

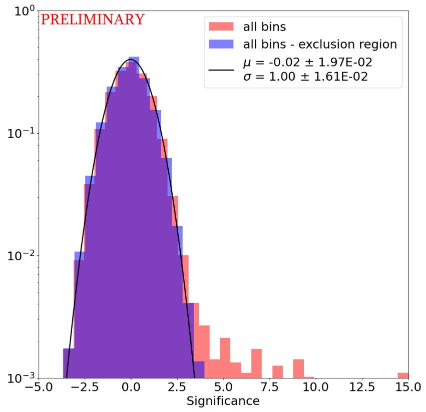

(b) Markarian-421 significance distribution. Note that the background significance is a standard normal distribution while the "all bins" distribution has a high-significance tail. This is what we expect to see from a significance distribution for a statistically-significant gamma-ray source detection.

Figure 5: *Markarian-421 significance analysis*

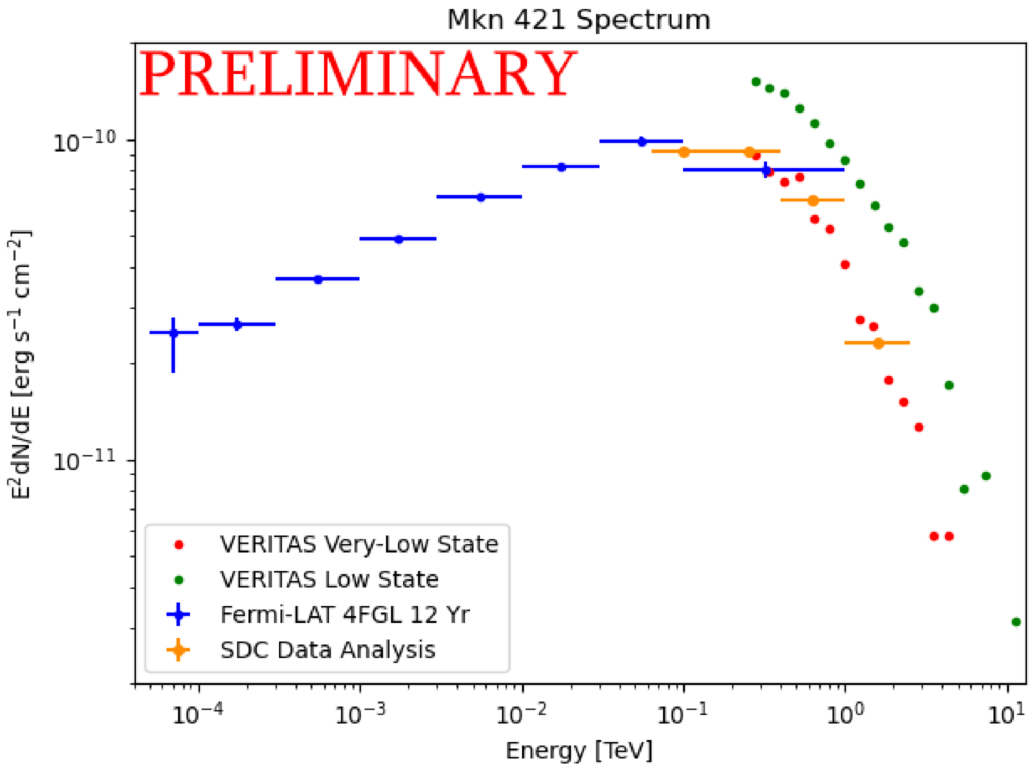

Figure 6: *Markarian-421 flux spectrum compared to VERITAS and Fermi-LAT flux data.*

Furthermore, the resulting flux spectrum from the spectral analysis can be found in 6. This is compared with Markarian-421 spectral analyses from the *VERITAS* collaboration [32] and *Fermi-LAT* data [5]. As we can see, the two spectra quantitatively agree for the 10^{-1} TeV to 10^{2} TeV range.

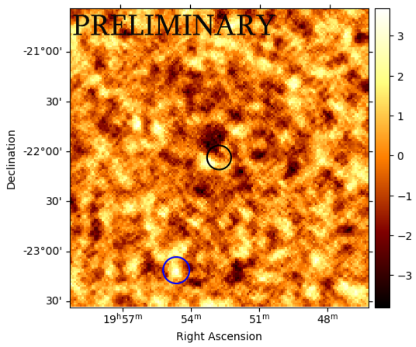

(a) Sagittarius-2 significance map for a point-source analysis. The peak significance (blue circle) is 3.7σ*. The black circle represents the integration region.*

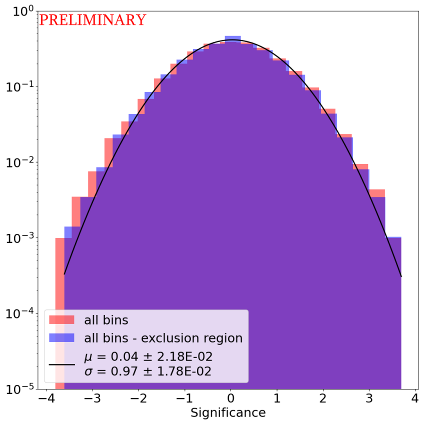

(b) Sagittarius-2 significance distribution for point-source analysis. Note that the background significance forms an expected normal distribution.

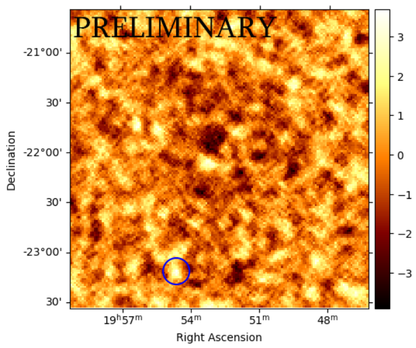

(c) Sagittarius-2 significance map for an extended-source analysis. The peak significance (circled) is 3.6σ*.*

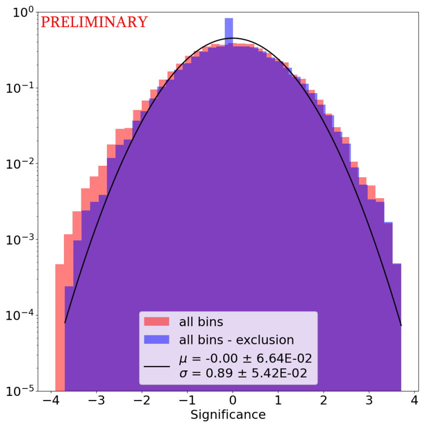

(d) Sagittarius-2 significance distribution for extended-source analysis.

Figure 7: *Sagittarius-2 significance analysis*

3.2 Sagittarius 2

The first dwarf spheroidal galaxy we analyzed is Sagittarius-2 with icrs coordinates of 298.2 deg ra and -22.07 deg dec. The significance map for the point-source analysis and related distribution can be found in Figures 7a and 7b. Furthermore, the extended-source analysis and related distribution can be found in Figures 7c and 7d, respectively. The peak significance values for both are $\approx 3.7\sigma$. Figure 8 illustrates the flux spectrum for Sagittarius-2. After applying a standard power law fit, the only upper limit found by the flux estimator has a flux value of 1.447×10^{-13} TeV cm$\hat{-}$2 s$\hat{-}$1 in the 0.079 TeV to 0.220 TeV bin.

3.3 Dark Matter Subhalo

For the galactic DM halo source, the SDC dataset has no wobble, so we use the analysis techniques described in 2 at a 0.5° displacement from each source position.

For the galactic dark matter subhalo, with icrs coordinates of 72.3 deg ra and -44.8 deg dec, the significance maps with related significance distributions are found in Figures 9d, 9c, 9b, and 9a. This covers both a point-source and extended-source analysis. Both analyses have a peak significance value of 4.0σ within the source region. Furthermore, Figure 10 displays the flux spectrum upper limits. The first upper limit, in the 0.369 TeV energy bin, has a flux of

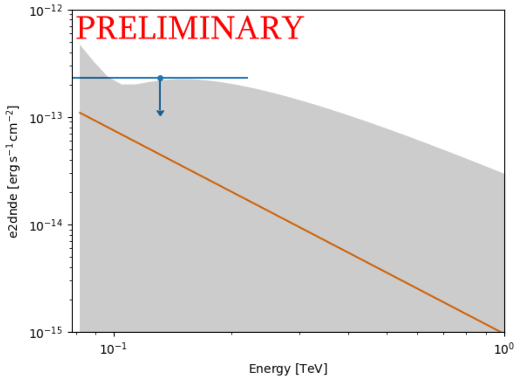

Figure 8: *Sagittarius-2 flux spectrum. Flux upper limit of* 1.447×10^{-13} *TeV cm-ˆ2 s-ˆ1 with a significance of* 0.485 *for the* 0.132 *TeV bin.*

1.355×10^{-13} TeV cm-ˆ2 s-ˆ1 with a significance of 0.977. The second, in the 1.034 TeV bin, has a flux value of 3.402×10^{-14} TeV cm-ˆ2 s-ˆ1 with a significance of 0.28σ.

3.4 Willman-1

The final source we analyze is Willman-1 with icrs coordinates of 162.33 deg ra and 51.049 deg dec. For the Willman I source, we perform a spectral and significance analysis using the methods described in 2. We perform a significance analysis using both a point-source integration radius and a slightly-extended integration radius of 0.10 deg. Furthermore, we perform two more extended-source analyses: an extraction region of 0.15 deg and an extraction region of 0.20 deg. For the significance analyses, we take the average peak significance for all four maps. Each peak significance is labeled on each map. The significance values have a range of 0.8σ from a minimum significance of 5.0σ to 5.8σ. We find a positive gamma-ray detection with an average significance stat of 5.5σ. Furthermore, each significance distribution is displayed with its related significance map. We can tell from the distribution plot that there is likely some analytical error causing an uneven significance distribution. While there is a possibility that the source may be further extended, it is highly unlikely due to the extended source analyses we have performed on the source. Further analytical investigation and likely debugging will be necessary to confirm. The distribution becomes more normal as the correlation radius decreases. The significance maps and their related significance distributions are shown in Figures 13b, 13a, 12b, 12a, 15b, 15a, 14b, and 14a.

What's more, the flux spectrum for Willman-1 is shown in Figure 11. As illustrated in 1, we fit an exponential cutoff power law model to Willman-1 with a fit statistic (wstat) of 2.93. The flux estimator gives us a $> 5\sigma$ significance for the spectrum within the 1.7 TeV to 4.9 TeV energy bin. Within this bin, we find a flux value of $(1.394 \times 10^{-13} \pm 2.948 \times 10^{-14})$ TeV cm-ˆ2 s-ˆ1 with significance value 5.5σ. Furthermore, the 1.0 TeV bin has a flux value of $(6.763 \times 10^{-14} \pm 3.224 \times 10^{-14})$ TeV cm-ˆ2 s-ˆ1 with a significance of 2.1σ and the 8.1 TeV has a flux value of $(4.768 \times 10^{-14} \pm 1.942 \times 10^{-14})$ TeV cm-ˆ2 s-ˆ1 with a significance of 2.9. It is surprising that we see a $> 5\sigma$ detection for Willman-1 because previous analyses of the source find no evidence for gamma-ray emissions from Willman-1 [9]. However, this is nonetheless a simulated dataset, so it is possible. Plus, it is worth noting that the same analytical error as we see in the significance maps may be plaguing the spectral analysis. Further analysis will be needed to verify these flux points.

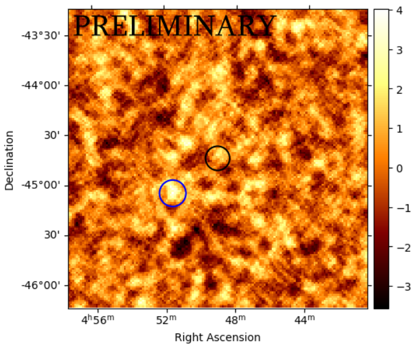

(a) *DM halo significance map for a point-source analysis. The peak significance (circled) is* 4.0σ*.*

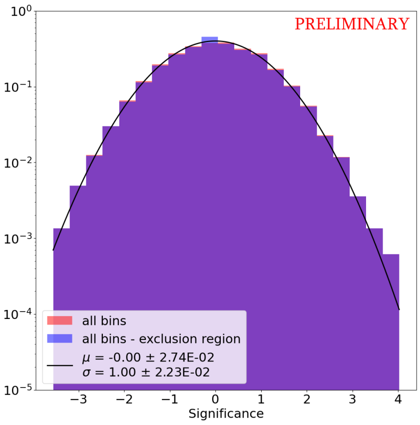

(b) *DM halo significance distribution for point-source analysis.*

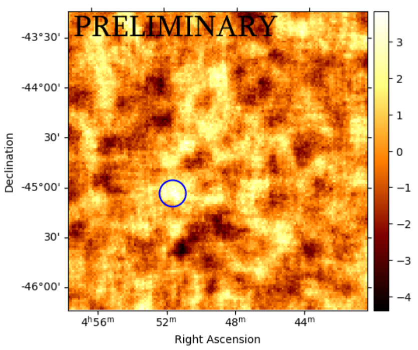

(c) *DM halo significance map for an extended-source analysis. The peak significance (circled) is* 4.0σ*.*

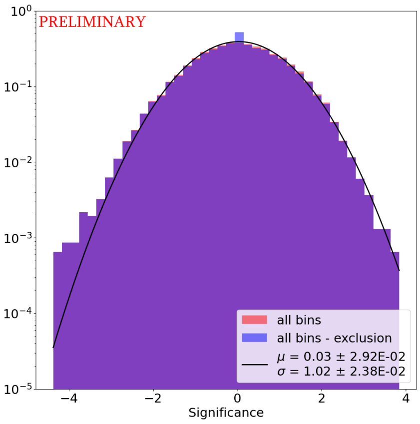

(d) *DM halo significance distribution for extended-source analysis.*

Figure 9: *Second DM halo significance analysis*

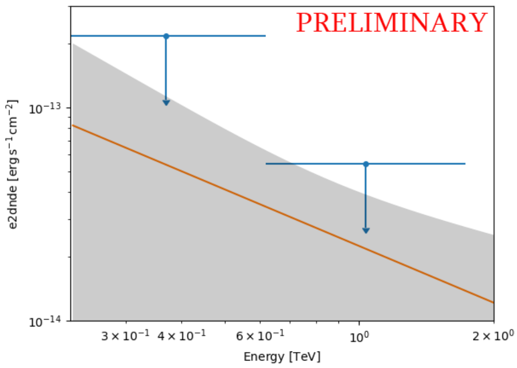

Figure 10: *DM halo source flux spectrum.*

4 Summary and Conclusions

Over the summer, I learned about the process behind analyzing VHE gamma rays. I studied different gamma-ray sources, including active galactic nuclei, a galactic DM subhalo, and extra-galactic DM-heavy dwarf spheroidal galaxies. I learned about different processes that accelerate particles, such as synchrotron radiation and inverse-Compton scattering. Additionally, I gained a deeper understanding of the reactions that occur in the atmosphere that allow us to detect gamma rays using IACTs. I studied the *VERITAS* and *CTAO* instruments, how they collect data from gamma-ray emissions, and how we can read the data they give us. In addition, I learned about dark matter and the different possible models that we can attempt to detect, such as WIMPs or axions. Additionally, I gained a grasp on indirect detection of WIMPs through dark matter annihilation or decay. I learned about *CTAO* and Gammapy, and gained experience using the Gammapy data analysis pipeline by analyzing DM sources. I gained in-depth experience with the gamma-ray analysis pipeline. From this, I learned and applied methods involving instrument IRFs, background modeling, and flux estimation. I comprehended the different techniques used in gamma-ray data analysis, such as reflected regions background estimation, backward-folding and forward-folding algorithms, and fitting models. Over the course of my project, I used the Second SDC data to compare simulated data with real, analyzed data for the Markarian-421 source. Once I had an effective data analysis pipeline, I construct flux spectra and significance maps for four DM sources using standard analytical methods. I surprisingly detect Willman-1 as a gamma-ray source with a significance of 5.5σ using backward-folding excess estimation and forward-folding flux estimation. The other three DM sources show no evidence of gamma-ray emission, but we find the flux upper-limits and significance peaks for each. Further analysis of the Second SDC data will allow us to further refine the Gammapy data analysis pipeline. An extension of this project may be to compare the results of these analyses with real DM upper limits. In addition, a more in-depth Gammapy data analysis pipeline may be constructed, and the documentation may be updated or amended with the suggestion of my notes and comments.

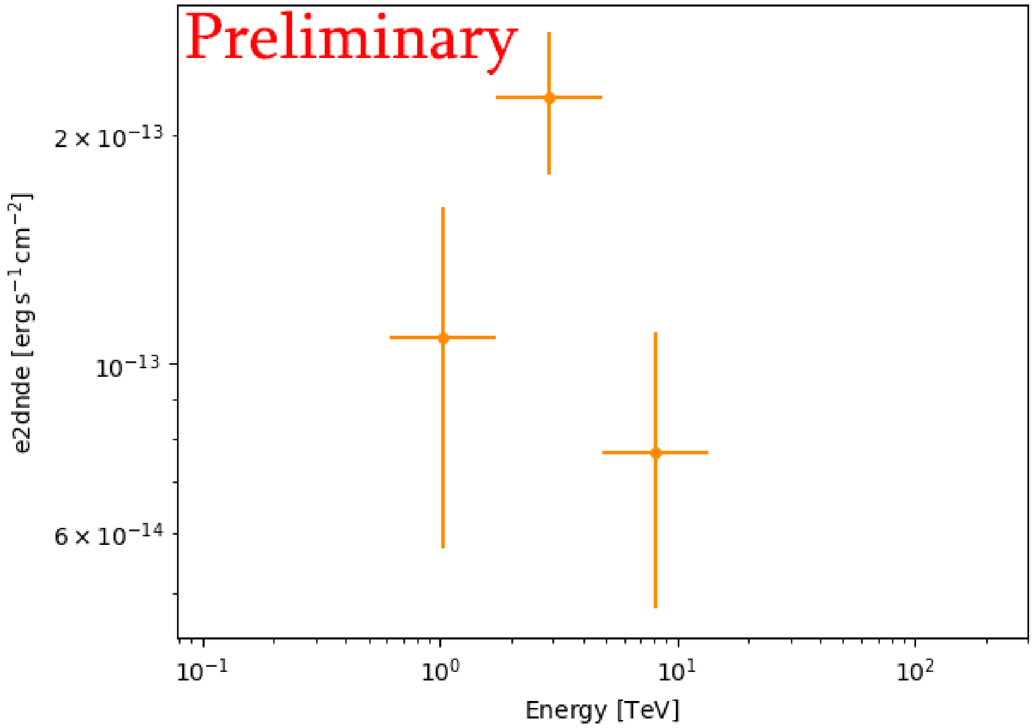

Figure 11: *The flux spectrum for Willman-1. Note that we see three solid flux points. However, further analysis will be necessary to confirm these flux points beyond the possibility of statistical error.*

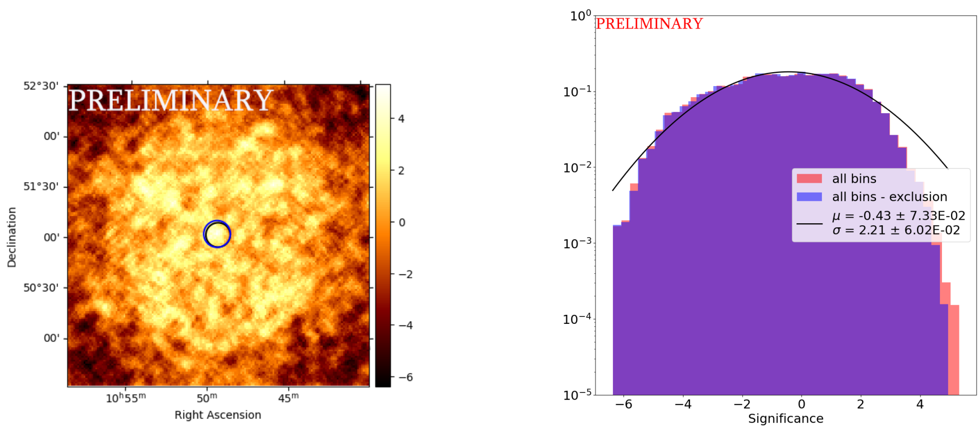

(a) *Willman-1 significance map for a point-source (extraction radius* = 0.07 deg *analysis. The significance peak has a value of* 5.0σ

(b) *Willman-1 significance distribution for a point-source analysis*

Figure 12: *Willman-1 high-level, point-source significance analysis.*

5 Acknowledgements

This material is based upon work supported by the National Science Foundation under Grant No. PHY-2349438. In addition, *VERITAS* and *CTAO* research at Barnard College is supported by NSF Grant No. PHY-2110497. Thank you to Prof. Reshmi Mukherjee, Dr. Ruo yu Shang, and the rest of the *VERITAS* group for your guidance and support throughout this project. Thank you to Zach Curtis-Ginsburg and Matthew Lundy for your assistance in debugging and in verifying results. Thank you to Prof. Reshmi Mukherjee, Prof. Georgia Karagiorgi, and Amy Garwood for administrating the program and inviting us all to participate. Finally, thank you to

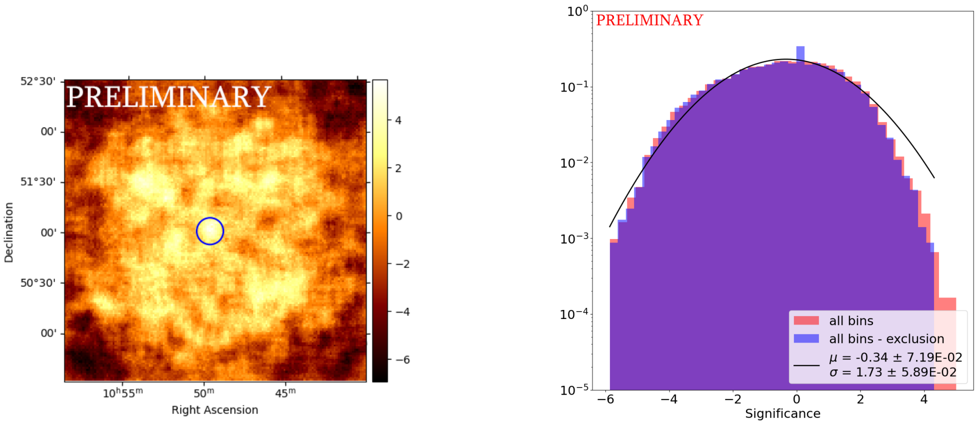

(a) *Willman-1 significance map for a slightly-extended-source (extraction radius* $= 0.10\,\mathrm{deg}$*) analysis. The significance peak has a value of* 5.6σ*.*

(b) *Willman-1 distribution map for a slightly-extended-source analysis.*

Figure 13: *Willman-1 high-level, slightly-extended-source significance analysis.*

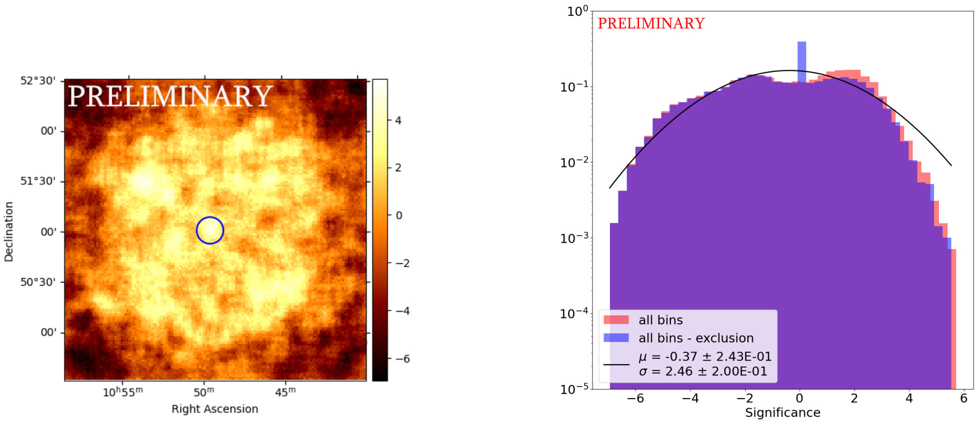

(a) *Willman-1 significance map for a moderately-extended (extraction radius* $= 0.15\,\mathrm{deg}$*) source analysis. The significance peak has a value of* 5.6σ*.*

(b) *Willman-1 distribution map for a moderately-extended source analysis.*

Figure 14: *Willman-1 low-level, point-source significance analysis.*

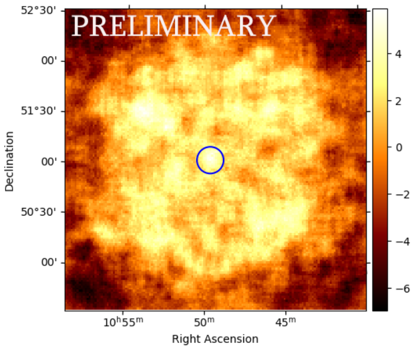

(a) Willman-1 significance map for a highly-extended (extraction radius = 0.20 deg) source analysis. The significance peak has a value of 5.8σ.

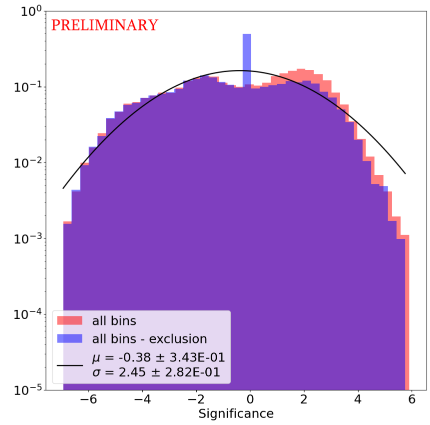

(b) Willman-1 distribution map for a low-level, extended-source analysis.

Figure 15: *Willman-1 low-level, extended-source significance analysis.*

Salma Ibrahim and the rest of the Columbia at Nevis Labs summer 2024 REU group for being great coworkers, roommates, and friends throughout the program.

References

[1] A. U. Abeysekara, A. Albert, R. Alfaro, C. Alvarez, J. D. Álvarez, R. Arceo, J. C. Arteaga-Velázquez, H. A. Ayala Solares, A. S. Barber, N. Bautista-Elivar, A. Becerril, E. Belmont-Moreno, S. Y. BenZvi, D. Berley, J. Braun, C. Brisbois, K. S. Caballero-Mora, T. Capistrán, A. Carramiñana, S. Casanova, M. Castillo, U. Cotti, J. Cotzomi, S. Coutiño de León, E. de la Fuente, C. De León, T. DeYoung, B. L. Dingus, M. A. DuVernois, J. C. Díaz-Vélez, R. W. Ellsworth, D. W. Fiorino, N. Fraija, J. A. García-González, M. Gerhardt, A. González Munöz, M. M. González, J. A. Goodman, Z. Hampel-Arias, J. P. Harding, S. Hernandez, A. Hernandez-Almada, J. Hinton, C. M. Hui, P. Hüntemeyer, A. Iriarte, A. Jardin-Blicq, V. Joshi, S. Kaufmann, D. Kieda, A. Lara, R. J. Lauer, W. H. Lee, D. Lennarz, H. León Vargas, J. T. Linnemann, A. L. Longinotti, G. Luis Raya, R. Luna-García, R. López-Coto, K. Malone, S. S. Marinelli, O. Martinez, I. Martinez-Castellanos, J. Martínez-Castro, H. Martínez-Huerta, J. A. Matthews, P. Miranda-Romagnoli, E. Moreno, M. Mostafá, L. Nellen, M. Newbold, M. U. Nisa, R. Noriega-Papaqui, R. Pelayo, J. Pretz, E. G. Pérez-Pérez, Z. Ren, C. D. Rho, C. Rivière, D. Rosa-González, M. Rosenberg, E. Ruiz-Velasco, H. Salazar, F. Salesa Greus, A. Sandoval, M. Schneider, H. Schoorlemmer, G. Sinnis, A. J. Smith, R. W. Springer, P. Surajbali, I. Taboada, O. Tibolla, K. Tollefson, I. Torres, T. N. Ukwatta, L. Villaseñor, T. Weisgarber, S. Westerhoff, I. G. Wisher, J. Wood, T. Yapici, G. B. Yodh, P. W. Younk, A. Zepeda, and H. Zhou. Observation of the crab nebula with the hawc gamma-ray observatory. *The Astrophysical Journal*, 843(1):39, June 2017.

[2] Fabio Acero, Juan Bernete, Noah Biederbeck, Julia Djuvsland, Axel Donath, Kirsty Feijen, Stefan Furse, Claudio Galelli, Bruno Khalifi, Jana Konrad, Paula Kornecki, Maximilian Linhoff, Kurt McKee, Simone Mender, Daniel Morcuende, Laura Olivera-Nieto, Fabio Pintore, Michael Punch, Maxime Regeard, Quentin Remy, Atreyee Sinha, Hanna Stapel, Katrin Streil, Regis Terrier, and Tim Unbehaun. Gammapy: Python toolbox for gamma-ray astronomy, 02 2024.

[3] A. Acharyya, C. B. Adams, P. Bangale, J. T. Bartkoske, P. Batista, W. Benbow, J. L. Christiansen, A. J. Chromey, A. Duerr, M. Errando, A. Falcone, Q. Feng, G. M. Foote, L. Fortson, A. Furniss, W. Hanlon, D. Hanna, O. Hervet, C. E. Hinrichs, J. Holder, T. B. Humensky, W. Jin, M. N. Johnson, P. Kaaret, M. Kertzman, D. Kieda, T. K. Kleiner, N. Korzoun, S. Kumar, M. J. Lang, M. Lundy, G. Maier, Conor E. McGrath, M. J. Millard, C. L. Mooney, P. Moriarty, R. Mukherjee, W. Ning, S. O'Brien, R. A. Ong, N. Park, M. Pohl, E. Pueschel, J. Quinn, P. L. Rabinowitz, K. Ragan, P. T. Reynolds, D. Ribeiro, E. Roache, J. L. Ryan, I. Sadeh, L. Saha, G. H. Sembroski, R. Shang, M. Splettstoesser, Donggeun Tak, A. K. Talluri, J. V. Tucci, V. V. Vassiliev, A. Weinstein, D. A. Williams, and S. L. Wong. An indirect search for dark matter with a combined analysis of dwarf spheroidal galaxies from veritas, 2024.

[4] A. Acharyya, A. Archer, P. Bangale, J. T. Bartkoske, P. Batista, M. Baumgart, W. Benbow, J. H. Buckley, A. Falcone, Q. Feng, J. P. Finley, G. M. Foote, L. Fortson, A. Furniss, G. Gallagher, W. F. Hanlon, O. Hervet, J. Hoang, J. Holder, T. B. Humensky, W. Jin, P. Kaaret, M. Kertzman, M. Kherlakian, D. Kieda, T. K. Kleiner, N. Korzoun, F. Krennrich, M. J. Lang, M. Lundy, G. Maier, C. E McGrath, P. Moriarty, S. O'Brien, R. A. Ong, K. Pfrang, M. Pohl, E. Pueschel, J. Quinn, K. Ragan, P. T. Reynolds, E. Roache, N. L. Rodd, J. L. Ryan, I. Sadeh, L. Saha, M. Santander, G. H. Sembroski, R. Shang, M. Splettstoesser, D. Tak, J. V. Tucci, V. V. Vassiliev, and D. A. Williams. Search for ultraheavy dark matter from observations of dwarf spheroidal galaxies with veritas. *The Astrophysical Journal*, 945(2):101, March 2023.

[5] M. Ajello, W. B. Atwood, M. Axelsson, R. Bagagli, M. Bagni, L. Baldini, D. Bastieri, F. Bellardi, R. Bellazzini, E. Bissaldi, E. D. Bloom, R. Bonino, J. Bregeon, A. Brez, P. Bruel, R. Buehler, S. Buson, R. A. Cameron, P. A. Caraveo, E. Cavazzuti, M. Ceccanti, S. Chen, C. C. Cheung, S. Ciprini, I. Cognard, J. Cohen-Tanugi, S. Cutini, F. D'Ammando, P. de la Torre Luque, F. de Palma, S. W. Digel, F. Dirirsa, N. Di Lalla, L. Di Venere, A. Domínguez, D. Fabiani, E. C. Ferrara, A. Fiori, G. Foglia, Y. Fukazawa, P. Fusco, F. Gargano, D. Gasparrini, M. Giroletti, T. Glanzman, D. Green, S. Griffin, M.-H. Grondin, J. E. Grove, L. Guillemot, S. Guiriec, M. Gustafsson, E. Hays, D. Horan, G. Jóhannesson, T. J. Johnson, T. Kamae, M. Kerr, M. Kuss, S. Larsson, L. Latronico, M. Lemoine-Goumard, J. Li, I. Liodakis, F. Longo, F. Loparco, M. N. Lovellette, P. Lubrano, S. Maldera, A. Manfreda, G. Martí-Devesa, M. N. Mazziotta, N. Menon, I. Mereu, M. Meyer, P. F. Michelson, M. Minuti, W. Mitthumsiri, T. Mizuno, M. Mongelli, M. E. Monzani, I. V. Moskalenko, M. Negro, E. Nuss, R. Ojha, M. Orienti, E. Orlando, A. Paccagnella, V. S. Paliya, D. Paneque, Z. Pei, J. S. Perkins, M. Pesce-Rollins, M. Pinchera, F. Piron, H. Poon, T. A. Porter, R. Primavera, G. Principe, J. L. Racusin, S. Rainò, R. Rando, B. Rani, E. Rapposelli, M. Razzano, S. Razzaque, A. Reimer, O. Reimer, J. J. Russell, N. Saggini, P. M. Saz Parkinson, N. Scolieri, D. Serini, C. Sgrò, E. J. Siskind, D. A. Smith, G. Spandre, P. Spinelli, D. J. Suson, H. Tajima, J. G. Thayer, D. J. Thompson, L. Tibaldo, D. F. Torres, G. Tosti, J. Valverde, L. Vigiani, and G. Zaharijas. Fermi large area telescope performance after 10 years of operation. *The Astrophysical Journal Supplement Series*, 256(1):12, September 2021.

[6] A. Albert, R. Alfaro, H. Ashkar, C. Alvarez, J. Álvarez, J. C. Arteaga-Velázquez, H. A. Ayala Solares, R. Arceo, J. A. Bellido, S. BenZvi, T. Bretz, C. A. Brisbois, A. M. Brown, F. Brun, K. S. Caballero-Mora, A. Carosi, A. Carramiñana, S. Casanova, P. M. Chadwick, G. Cotter, S. Coutiño De León, P. Cristofari, S. Dasso, E. de la Fuente, B. L. Dingus, P. Desiati, F. de O. Salles, V. de Souza, D. Dorner, J. C. Díaz-Vélez, J. A. García-González, M. A. DuVernois, G. Di Sciascio, K. Engel, H. Fleischhack, N. Fraija, S. Funk, J-F. Glicenstein, J. Gonzalez, M. M. González, J. A. Goodman, J. P. Harding, A. Haungs, J. Hinton, B. Hona, D. Hoyos, P. Huentemeyer, A. Iriarte, A. Jardin-Blicq, V. Joshi, S. Kaufmann, K. Kawata, S. Kunwar, J. Lefaucheur, J. P. Lenain, K. Link, R. López-Coto, V. Marandon, M. Mariotti, J. Martínez-Castro, H. Martínez-Huerta, M. Mostafá, A. Nayerhoda, L. Nellen, E. de Oña Wilhelmi, R. D. Parsons, B. Patricelli, A. Pichel, Q. Piel, E. Prandini, E. Pueschel, S. Procureur, A. Reisenegger, C. Rivière, J. Rodriguez, A. C. Rovero, G. Rowell, E. L. Ruiz-Velasco, A. Sandoval, M. Santander, T. Sako, T. K. Sako, K. Satalecka, H. Schoorlemmer, F. Schüssler, M. Seglar-Arroyo, A. J. Smith, S. Spencer, P. Surajbali, E. Tabachnick, A. M. Taylor, O. Tibolla, I. Torres, B. Vallage, A. Viana, J. J. Watson, T. Weisgarber, F. Werner, R. White, R. Wischnewski, R. Yang, A. Zepeda, and H. Zhou. Science case for a wide field-of-view very-high-energy gamma-ray observatory in the southern hemisphere, 2019.

[7] A. Albert, B. Anderson, K. Bechtol, A. Drlica-Wagner, M. Meyer, M. Sánchez-Conde, L. Strigari, M. Wood, T. M. C. Abbott, F. B. Abdalla, A. Benoit-Lévy, G. M. Bernstein, R. A. Bernstein, E. Bertin, D. Brooks, D. L. Burke, A. Carnero Rosell, M. Carrasco Kind, J. Carretero, M. Crocce, C. E. Cunha, C. B. D'Andrea, L. N. da Costa, S. Desai, H. T. Diehl, J. P. Dietrich, P. Doel, T. F. Eifler, A. E. Evrard, A. Fausti Neto, D. A. Finley, B. Flaugher, P. Fosalba, J. Frieman, D. W. Gerdes, D. A. Goldstein, D. Gruen, R. A. Gruendl, K. Honscheid, D. J. James, S. Kent, K. Kuehn, N. Kuropatkin, O. Lahav, T. S. Li, M. A. G. Maia, M. March, J. L. Marshall, P. Martini, C. J. Miller, R. Miquel, E. Neilsen, B. Nord, R. Ogando, A. A. Plazas, K. Reil, A. K. Romer, E. S. Rykoff, E. Sanchez, B. Santiago, M. Schubnell, I. Sevilla-Noarbe, R. C. Smith, M. Soares-Santos, F. Sobreira, E. Suchyta, M. E. C. Swanson, G. Tarle, V. Vikram, A. R. Walker, R. H. Wechsler, Fermi-LAT Collaboration, and DES Collaboration. Searching for Dark Matter Annihilation in Recently Discovered Milky Way Satellites with Fermi-Lat. *apj*, 834(2):110, January 2017.

[8] J. Aleksić, S. Ansoldi, L. A. Antonelli, P. Antoranz, A. Babic, P. Bangale, M. Barceló, J. A. Barrio, J. Becerra González, W. Bednarek, E. Bernardini, B. Biasuzzi, A. Biland, M. Bitossi, O. Blanch, S. Bonnefoy, G. Bonnoli, F. Borracci, T. Bretz, E. Carmona, A. Carosi, R. Cecchi, P. Colin, E. Colombo, J. L. Contreras, D. Corti, J. Cortina, S. Covino, P. Da Vela, F. Dazzi, A. De Angelis, G. De Caneva, B. De Lotto, E. de Oña Wilhelmi, C. Delgado Mendez, A. Dettlaff, D. Dominis Prester, D. Dorner, M. Doro, S. Einecke, D. Eisenacher, D. Elsaesser, D. Fidalgo, D. Fink, M. V. Fonseca, L. Font, K. Frantzen, C. Fruck, D. Galindo, R. J. García López, M. Garczarczyk, D. Garrido Terrats, M. Gaug, G. Giavitto, N. Godinović, A. González Muñoz, S. R. Gozzini, W. Haberer, D. Hadasch, Y. Hanabata, M. Hayashida, J. Herrera, D. Hildebrand, J. Hose, D. Hrupec, W. Idec, J. M. Illa, V. Kadenius, H. Kellermann, M. L. Knoetig, K. Kodani, Y. Konno, J. Krause, H. Kubo, J. Kushida, A. La Barbera, D. Lelas, J. L. Lemus, N. Lewandowska, E. Lindfors, S. Lombardi, F. Longo, M. López, R. López-Coto, A. López-Oramas, A. Lorca, E. Lorenz, I. Lozano, M. Makariev, K. Mallot, G. Maneva, N. Mankuzhiyil, K. Mannheim, L. Maraschi, B. Marcote, M. Mariotti, M. Martínez, D. Mazin, U. Menzel, J. M. Miranda, R. Mirzoyan, A. Moralejo, P. Munar-Adrover, D. Nakajima, M. Negrello, V. Neustroev, A. Niedzwiecki, K. Nilsson, K. Nishijima, K. Noda, R. Orito, A. Overkemping, S. Paiano, M. Palatiello, D. Paneque, R. Paoletti, J. M. Paredes, X. Paredes-Fortuny, M. Persic, J. Poutanen, P. G. Prada Moroni, E. Prandini, I. Puljak, R. Reinthal, W. Rhode, M. Ribó, J. Rico, J. Rodriguez Garcia, S. Rügamer, T. Saito, K. Saito, K. Satalecka, V. Scalzotto, V. Scapin, C. Schultz, J. Schlammer, S. Schmidl, T. Schweizer, S. N. Shore, A. Sillanpää, J. Sitarek, I. Snidaric, D. Sobczynska, F. Spanier, A. Stamerra, T. Steinbring, J. Storz, M. Strzys, L. Takalo, H. Takami, F. Tavecchio, L. A. Tejedor, P. Temnikov, T. Terzić, D. Tescaro, M. Teshima, J. Thaele, O. Tibolla, D. F. Torres, T. Toyama, A. Treves, P. Vogler, H. Wetteskind, M. Will, and R. Zanin. The major upgrade of the MAGIC telescopes, Part II: A performance study using observations of the Crab Nebula. *Astroparticle Physics*, 72:76–94, January 2016.

[9] S. Archambault, A. Archer, W. Benbow, R. Bird, E. Bourbeau, T. Brantseg, M. Buchovecky, J. H. Buckley, V. Bugaev, K. Byrum, M. Cerruti, J. L. Christiansen, M. P. Connolly, W. Cui, M. K. Daniel, Q. Feng, J. P. Finley, H. Fleischhack, L. Fortson, A. Furniss, A. Geringer-Sameth, S. Griffin, J. Grube, M. Hütten, N. Håkansson, D. Hanna, O. Hervet, J. Holder, G. Hughes, B. Hummensky, C. A. Johnson, P. Kaaret, P. Kar, N. Kelley-Hoskins, M. Kertzman, D. Kieda, S. Koushiappas, M. Krause, F. Krennrich, M. J. Lang, T. T. Y. Lin, S. McArthur, P. Moriarty, R. Mukherjee, D. Nieto, S. O'Brien, R. A. Ong, A. N. Otte, N. Park, M. Pohl, A. Popkow, E. Pueschel, J. Quinn, K. Ragan, P. T. Reynolds, G. T. Richards, E. Roache, C. Rulten, I. Sadeh, M. Santander, G. H. Sembroski, K. Shahinyan, A. W. Smith, D. Staszak, I. Telezhinsky, S. Trepanier, J. V. Tucci, J. Tyler, S. P. Wakely, A. Weinstein, P. Wilcox, D. A. Williams, and B. Zitzer. Dark matter constraints from a joint analysis of dwarf spheroidal galaxy observations with veritas. *Phys. Rev. D*, 95:082001, Apr 2017.

[10] Astropy Collaboration, A. M. Price-Whelan, B. M. Sipőcz, H. M. Günther, P. L. Lim, S. M. Crawford, S. Conseil, D. L. Shupe, M. W. Craig, N. Dencheva, A. Ginsburg, J. T. Vand erPlas, L. D. Bradley, D. Pérez-Suárez, M. de Val-Borro, T. L. Aldcroft, K. L. Cruz, T. P. Robitaille, E. J. Tollerud, C. Ardelean, T. Babej, Y. P. Bach, M. Bachetti, A. V. Bakanov, S. P. Bamford, G. Barentsen, P. Barmby, A. Baumbach, K. L. Berry, F. Biscani, M. Boquien, K. A. Bostroem, L. G. Bouma, G. B. Brammer, E. M. Bray, H. Breytenbach, H. Buddelmeijer, D. J. Burke, G. Calderone, J. L. Cano Rodríguez, M. Cara, J. V. M. Cardoso, S. Cheedella, Y. Copin, L. Corrales, D. Crichton, D. D'Avella, C. Deil, É. Depagne, J. P. Dietrich, A. Donath, M. Droettboom, N. Earl, T. Erben, S. Fabbro, L. A. Ferreira, T. Finethy, R. T. Fox, L. H. Garrison, S. L. J. Gibbons, D. A. Goldstein, R. Gommers, J. P. Greco, P. Greenfield, A. M. Groener, F. Grollier, A. Hagen, P. Hirst, D. Homeier, A. J. Horton, G. Hossein-

zadeh, L. Hu, J. S. Hunkeler, Ž. Ivezić, A. Jain, T. Jenness, G. Kanarek, S. Kendrew, N. S. Kern, W. E. Kerzendorf, A. Khvalko, J. King, D. Kirkby, A. M. Kulkarni, A. Kumar, A. Lee, D. Lenz, S. P. Littlefair, Z. Ma, D. M. Macleod, M. Mastropietro, C. McCully, S. Montagnac, B. M. Morris, M. Mueller, S. J. Mumford, D. Muna, N. A. Murphy, S. Nelson, G. H. Nguyen, J. P. Ninan, M. Nöthe, S. Ogaz, S. Oh, J. K. Parejko, N. Parley, S. Pascual, R. Patil, A. A. Patil, A. L. Plunkett, J. X. Prochaska, T. Rastogi, V. Reddy Janga, J. Sabater, P. Sakurikar, M. Seifert, L. E. Sherbert, H. Sherwood-Taylor, A. Y. Shih, J. Sick, M. T. Silbiger, S. Singanamalla, L. P. Singer, P. H. Sladen, K. A. Sooley, S. Sornarajah, O. Streicher, P. Teuben, S. W. Thomas, G. R. Tremblay, J. E. H. Turner, V. Terrón, M. H. van Kerkwijk, A. de la Vega, L. L. Watkins, B. A. Weaver, J. B. Whitmore, J. Woillez, V. Zabalza, and Astropy Contributors. The Astropy Project: Building an Open-science Project and Status of the v2.0 Core Package. *apj*, 156(3):123, September 2018.

[11] Astropy Collaboration, Adrian M. Price-Whelan, Pey Lian Lim, Nicholas Earl, Nathaniel Starkman, Larry Bradley, David L. Shupe, Aarya A. Patil, Lia Corrales, C. E. Brasseur, Maximilian N"othe, Axel Donath, Erik Tollerud, Brett M. Morris, Adam Ginsburg, Eero Vaher, Benjamin A. Weaver, James Tocknell, William Jamieson, Marten H. van Kerkwijk, Thomas P. Robitaille, Bruce Merry, Matteo Bachetti, H. Moritz G"unther, Thomas L. Aldcroft, Jaime A. Alvarado-Montes, Anne M. Archibald, Attila B'odi, Shreyas Bapat, Geert Barentsen, Juanjo Baz'an, Manish Biswas, M'ed'eric Boquien, D. J. Burke, Daria Cara, Mihai Cara, Kyle E. Conroy, Simon Conseil, Matthew W. Craig, Robert M. Cross, Kelle L. Cruz, Francesco D'Eugenio, Nadia Dencheva, Hadrien A. R. Devillepoix, J"org P. Dietrich, Arthur Davis Eigenbrot, Thomas Erben, Leonardo Ferreira, Daniel Foreman-Mackey, Ryan Fox, Nabil Freij, Suyog Garg, Robel Geda, Lauren Glattly, Yash Gondhalekar, Karl D. Gordon, David Grant, Perry Greenfield, Austen M. Groener, Steve Guest, Sebastian Gurovich, Rasmus Handberg, Akeem Hart, Zac Hatfield-Dodds, Derek Homeier, Griffin Hosseinzadeh, Tim Jenness, Craig K. Jones, Prajwel Joseph, J. Bryce Kalmbach, Emir Karamehmetoglu, Mikolaj Kaluszy'nski, Michael S. P. Kelley, Nicholas Kern, Wolfgang E. Kerzendorf, Eric W. Koch, Shankar Kulumani, Antony Lee, Chun Ly, Zhiyuan Ma, Conor MacBride, Jakob M. Maljaars, Demitri Muna, N. A. Murphy, Henrik Norman, Richard O'Steen, Kyle A. Oman, Camilla Pacifici, Sergio Pascual, J. Pascual-Granado, Rohit R. Patil, Gabriel I. Perren, Timothy E. Pickering, Tanuj Rastogi, Benjamin R. Roulston, Daniel F. Ryan, Eli S. Rykoff, Jose Sabater, Parikshit Sakurikar, Jes'us Salgado, Aniket Sanghi, Nicholas Saunders, Volodymyr Savchenko, Ludwig Schwardt, Michael Seifert-Eckert, Albert Y. Shih, Anany Shrey Jain, Gyanendra Shukla, Jonathan Sick, Chris Simpson, Sudheesh Singanamalla, Leo P. Singer, Jaladh Singhal, Manodeep Sinha, Brigitta M. SipHocz, Lee R. Spitler, David Stansby, Ole Streicher, Jani Sumak, John D. Swinbank, Dan S. Taranu, Nikita Tewary, Grant R. Tremblay, Miguel de Val-Borro, Samuel J. Van Kooten, Zlatan Vasovi'c, Shresth Verma, Jos'e Vin'icius de Miranda Cardoso, Peter K. G. Williams, Tom J. Wilson, Benjamin Winkel, W. M. Wood-Vasey, Rui Xue, Peter Yoachim, Chen Zhang, Andrea Zonca, and Astropy Project Contributors. The Astropy Project: Sustaining and Growing a Community-oriented Open-source Project and the Latest Major Release (v5.0) of the Core Package. *apj*, 935(2):167, August 2022.

[12] Astropy Collaboration, T. P. Robitaille, E. J. Tollerud, P. Greenfield, M. Droettboom, E. Bray, T. Aldcroft, M. Davis, A. Ginsburg, A. M. Price-Whelan, W. E. Kerzendorf, A. Conley, N. Crighton, K. Barbary, D. Muna, H. Ferguson, F. Grollier, M. M. Parikh, P. H. Nair, H. M. Unther, C. Deil, J. Woillez, S. Conseil, R. Kramer, J. E. H. Turner, L. Singer, R. Fox, B. A. Weaver, V. Zabalza, Z. I. Edwards, K. Azalee Bostroem, D. J. Burke, A. R. Casey, S. M. Crawford, N. Dencheva, J. Ely, T. Jenness, K. Labrie, P. L. Lim, F. Pierfederici, A. Pontzen, A. Ptak, B. Refsdal, M. Servillat, and O. Streicher. Astropy: A community Python package for astronomy. *aap*, 558:A33, October 2013.

[13] Berge, D., Funk, S., and Hinton, J. Background modelling in very-high-energy γ-ray astronomy. *A&A*, 466(3):1219–1229, 2007.

[14] Zhen Cao, D. della Volpe, Siming Liu, Editors, :, Xiaojun Bi, Yang Chen, B. D'Ettorre Piazzoli, Li Feng, Huanyu Jia, Zhuo Li, Xinhua Ma, Xiangyu Wang, Xiao Zhang, External Referees, :, Xiushu Qie, Hongbo Hu, Internal Referees, :, Alejandro Sáiz, Ruizhi Yang, Contributors, :, Andrea Addazi, Konstantin Belotsky, Vitaly Beylin, Yu-Jiang Bi, Ming-Jun Che, Song-Zhan Chen, Yao-Dong Cheng, Andrea Chiavassa, Marco Cirelli, Giuseppe Di Sciascio, Arman Esmaili, Kun Fang, Nicolao Fornengo, Quanbu Gou, Yi-Qing Guo, Qingyu Gan, Guang-Hua Gong, Min-Hao Gu, Haoning He, Hui-Hai He, Chao Hou, Xing-Tao Huang, Wen-Hao Huang, Michael Kachekriess, Maxim Khlopov, Vladimir Korchagin, Alexander Korochkin, Vladimir Kuksa, Leonid T. Ksenofontov, Ye Liu, Ruo-Yu Liu, Cheng Liu, Antonino Marciano, Olivier Martineau-Huynh, Diane Martraire, Lingling Ma, Andrii Neronov, Paolo Panci, Roman Pasechnick, David Ruffolo, Alexander Sakharov, Filippo Sala, Dimiri Semikoz, Oleg Shchegolev, Pasquale Dario Serpico, Xiang-Dong Sheng, Yuri V. Stenkin, P. H. Thomas Tam, Silvia Vernetto, Piero Vallania, Nikolay Volchanskiy, Zhongxiang Wang, Kai Wang, Xiang-Yu Wang, Han-Rong Wu, Chao-Yong Wu, Sha Wu, Gang Xiao, Rui zhi Yang, Dahai Yan, Zhi-Guo Yao, Pengfei Yin, Qiang Yuan, Xiao Zhang, Houdun Zeng, Shou-Shan Zhang, Yi Zhang, Xunxiu Zhou, Hui Zhu, and Xiong Zuo. The large high altitude air shower observatory (lhaaso) science book (2021 edition), 2022.

[15] Marco Cirelli, Gennaro Corcella, Andi Hektor, Gert Hütsi, Mario Kadastik, Paolo Panci, Martti Raidal, Filippo Sala, and Alessandro Strumia. Pppc 4 dm id: a poor particle physicist cookbook for dark matter indirect detection. *Journal of Cosmology and Astroparticle Physics*, 2011(03):051, mar 2011.

[16] HEGRA Collaboration and A. Daum et al. First results on the performance of the hegra iact array, 1997.

[17] Sara Coutiño de León, Alberto Carramiñana Alonso, Daniel Rosa-González, and Anna Lia Longinotti. Spectral analysis of the blazars markarian 421 and markarian 501 with the hawc gamma-ray observatory, 2019.

[18] A. Domínguez, J. R. Primack, D. J. Rosario, F. Prada, R. C. Gilmore, S. M. Faber, D. C. Koo, R. S. Somerville, M. A. Pérez-Torres, P. Pérez-González, J.-S. Huang, M. Davis, P. Guhathakurta, P. Barmby, C. J. Conselice, M. Lozano, J. A. Newman, and M. C. Cooper. Extragalactic background light inferred from aegis galaxy-sed-type fractions: Ebl from aegis galaxy-sed-type fractions. *Monthly Notices of the Royal Astronomical Society*, 410(4):2556–2578, October 2010.

[19] Axel Donath, Régis Terrier, Quentin Remy, Atreyee Sinha, Cosimo Nigro, Fabio Pintore, Bruno Khélifi, Laura Olivera-Nieto, Jose Enrique Ruiz, Kai Brügge, Maximilian Linhoff, Jose Luis Contreras, Fabio Acero, Arnau Aguasca-Cabot, David Berge, Pooja Bhattacharjee, Johannes Buchner, Catherine Boisson, David Carreto Fidalgo, Andrew Chen, Mathieu de Bony de Lavergne, José Vinicius de Miranda Cardoso, Christoph Deil, Matthias Füßling, Stefan Funk, Luca Giunti, Jim Hinton, Léa Jouvin, Johannes King, Julien Lefaucheur, Marianne Lemoine-Goumard, Jean-Philippe Lenain, Rubén López-Coto, Lars Mohrmann, Daniel Morcuende, Sebastian Panny, Maxime Regeard, Lab Saha, Hubert Siejkowski, Aneta Siemiginowska, Brigitta M. Sip"ocz, Tim Unbehaun, Christopher van Eldik, Thomas Vuillaume, and Roberta Zanin. Gammapy: A python package for gamma-ray astronomy. *A&A*, 678:A157, 2023.

[20] Carmelo Evoli. The cosmic-ray energy spectrum, December 2020.

[21] Katherine Garrett and Gintaras Duda. Dark matter: A primer. *Advances in Astronomy*, 2011:1–22, 2011.

[22] Charles R. Harris, K. Jarrod Millman, Stéfan J. van der Walt, Ralf Gommers, Pauli Virtanen, David Cournapeau, Eric Wieser, Julian Taylor, Sebastian Berg, Nathaniel J. Smith, Robert Kern, Matti Picus, Stephan Hoyer, Marten H. van Kerkwijk, Matthew Brett, Allan Haldane, Jaime Fernández del Río, Mark Wiebe, Pearu Peterson, Pierre Gérard-Marchant, Kevin Sheppard, Tyler Reddy, Warren Weckesser, Hameer Abbasi, Christoph Gohlke, and Travis E. Oliphant. Array programming with NumPy. *Nature*, 585(7825):357–362, September 2020.

[23] Werner Hofmann and Roberta Zanin. The cherenkov telescope array, 2023.

[24] Markus Holler et al. Observations of the Crab Nebula with H.E.S.S. Phase II. *PoS*, ICRC2015:847, 2016.

[25] F. James and M. Roos. Minuit: A System for Function Minimization and Analysis of the Parameter Errors and Correlations. *Comput. Phys. Commun.*, 10:343–367, 1975.

[26] Benjamin P. M. Laevens, Nicolas F. Martin, Edouard J. Bernard, Edward F. Schlafly, Branimir Sesar, Hans-Walter Rix, Eric F. Bell, Annette M. N. Ferguson, Colin T. Slater, William E. Sweeney, Rosemary F. G. Wyse, Avon P. Huxor, William S. Burgett, Kenneth C. Chambers, Peter W. Draper, Klaus W. Hodapp, Nicholas Kaiser, Eugene A. Magnier, Nigel Metcalfe, John L. Tonry, Richard J. Wainscoat, and Christopher Waters. Sagittarius II, Draco II and Laevens 3: Three New Milky Way Satellites Discovered in the Pan-STARRS 1 3π Survey. *apj*, 813(1):44, November 2015.

[27] T. P. Li and Y. Q. Ma. Analysis methods for results in gamma-ray astronomy. *apj*, 272:317–324, September 1983.

[28] Saverio Lombardi, L. A. Antonelli, C. Bigongiari, M. Cardillo, S. Gallozzi, J. G. Green, F. Lucarelli, and F. G. Saturni. Performance of the ASTRI Mini-Array at the Observatorio del Teide. *PoS*, ICRC2021:884, 2021.

[29] Nicolas Longeard, Nicolas Martin, Rodrigo A Ibata, Else Starkenburg, Pascale Jablonka, David S Aguado, Raymond G Carlberg, Patrick Côté, Jonay I González Hernández, Romain Lucchesi, Khyati Malhan, Julio F Navarro, Rubén Sánchez-Janssen, Guillaume F Thomas, Kim Venn, and Alan W McConnachie. The pristine dwarf-galaxy survey – iii. revealing the nature of the milky way globular cluster sagittarius ii. *Monthly Notices of the Royal Astronomical Society*, 503(2):2754–2762, March 2021.

[30] Nicolas Longeard, Nicolas Martin, Else Starkenburg, Rodrigo A. Ibata, Michelle L. M. Collins, Benjamin P. M. Laevens, Dougal Mackey, R. Michael Rich, David S. Aguado, Anke Arentsen, Pascale Jablonka, Jonay I. González Hernández, Julio F. Navarro, and Rubén Sánchez-Janssen. The Pristine Dwarf-Galaxy survey - II. In-depth observational study of the faint Milky Way satellite Sagittarius II. *mnras*, 491(1):356–377, January 2020.

[31] Conor McGrath. An indirect search for Dark Matter with a combined analysis of dwarf spheroidal galaxies from VERITAS. *PoS*, ICRC2023:1395, 2023.

[32] R. Mukherjee. Observing the energetic universe at very high energies with the veritas gamma ray observatory. *Advances in Space Research*, 62(10):2828–2844, 2018. Origins of Cosmic Rays.

[33] Daniel Nieto. Hunting for dark matter subhalos among the fermi-lat sources with veritas, 2015.

[34] M. Punch, C. W. Akerlof, M. F. Cawley, M. Chantell, D. J. Fegan, S. Fennell, J. A. Gaidos, J. Hagan, A. M. Hillas, Y. Jiang, A. D. Kerrick, R. C. Lamb, M. A. Lawrence, D. A. Lewis, D. I. Meyer, G. Mohanty, K. S. O'Flaherty, P. T. Reynolds, A. C. Rovero, M. S. Schubnell, G. Sembroski, T. C. Weekes, T. Whitaker, and C. Wilson. Detection of TeV photons from the active galaxy Markarian 421. *Nature*, 358(6386):477–478, August 1992.

[35] Pauli Virtanen, Ralf Gommers, Travis E. Oliphant, Matt Haberland, Tyler Reddy, David Cournapeau, Evgeni Burovski, Pearu Peterson, Warren Weckesser, Jonathan Bright, Stéfan J. van der Walt, Matthew Brett, Joshua Wilson, K. Jarrod Millman, Nikolay Mayorov, Andrew R. J. Nelson, Eric Jones, Robert Kern, Eric Larson, C J Carey, İlhan Polat, Yu Feng, Eric W. Moore, Jake VanderPlas, Denis Laxalde, Josef Perktold, Robert Cimrman, Ian Henriksen, E. A. Quintero, Charles R. Harris, Anne M. Archibald, Antônio H. Ribeiro, Fabian Pedregosa, Paul van Mulbregt, and SciPy 1.0 Contributors. SciPy 1.0: Fundamental Algorithms for Scientific Computing in Python. *Nature Methods*, 17:261–272, 2020.

[36] Beth Willman, Marla Geha, Jay Strader, Louis E. Strigari, Joshua D. Simon, Evan Kirby, Nhung Ho, and Alex Warres. Willman 1—A Probable Dwarf Galaxy with an Irregular Kinematic Distribution. *apj*, 142(4):128, October 2011.